



Entropy generation for spiral heat exchanger with considering NEPCM charging process using hybrid nanomaterial

Ahmad Shafee¹, M. Jafaryar², Metib Alghamdi³, Iskander Tlili^{4,5,a}

¹ Institute of Research and Development, Duy Tan University, Da Nang 550000, Vietnam

² Renewable Energy Systems and Nanofluid Applications in Heat Transfer Laboratory, Babol Noshirvani University of Technology, Babol, Iran

³ Department of Mathematics, Faculty of Science, King Khalid University, Abha 61413, Kingdom of Saudi Arabia

⁴ Department for Management of Science and Technology Development, Ton Duc Thang University, Ho Chi Minh City, Vietnam

⁵ Faculty of Applied Sciences, Ton Duc Thang University, Ho Chi Minh City, Vietnam

Received: 13 August 2019 / Accepted: 14 February 2020 / Published online: 5 March 2020

© Società Italiana di Fisica and Springer-Verlag GmbH Germany, part of Springer Nature 2020

Abstract In current unsteady simulation, charging of paraffin in an enclosure which is equipped with spiral pipe was scrutinized. Not only in paraffin but also in water inside the pipe, nanoparticles were dispersed to boost the thermal treatment. Outputs were reported in various stages in forms of irreversibility components. Increasing inlet velocity leads to higher liquid fraction which means better performance. As time increases, inlet velocity has lower effect on melting process. Increasing pumping power is beneficial only when time is lower than 20 min. Frictional irreversibility increases with time at initial time, and then, it reduces.

1 Introduction

Improving TES (thermal energy storage) can give us the opportunity to respond energy requests. This can grow the effectiveness of various energy technologies including solar thermal system. Environmental influence, fossil fuel resources and restricted energy supplies are the main problems that researchers are faced. Because of intermittent availability, high price of installation and maintenance, sustainable sources like wind and solar energy are required. Thermal energy storage can be an appropriate alternative solution for correcting the intermittency, and they are more efficient which can progress the wider application of the aforesaid sources [1–5]. One of the most frequently challenges with PCMs utilized in the applications of thermal energy storage is low thermal conductivity. This can pose to an imperfect discharging and charging procedures. Nanotechnology helps the researcher to solve this fault [6–19]. The efficiency of such systems is restricted in different temperatures through PCM, causing system overheating and substance failure. Phase change material is very practical in such engineering applications as water heating, electronic cooling, building heating, dry technology, air conditioning and solar energy systems [20–25]. Li et al. [26] scrutinized the transient discharging phenomena with help of nanomaterial. Sheikholeslami

^a e-mails: iskander.tlili@tdtu.edu.vn (corresponding author)

and Mahian [27] examined the impact of MHD on solidification in the presence of inorganic nanomaterial.

Numerically, the impact of HTF in a TES was analyzed by Agyenim et al. [28] who studied various configurations. Based on their results, the axial heat transfer can be ignored. Classic numerical approaches help scientist to simulate behavior of system before design step [29–55]. In addition, molecular modeling can show the nanomaterial behavior with more details [56,57]. PCM-LHTES systems involving simple pipe, circular finned pipe and pinned tube were simulated by Tay et al. [58] who found that the most efficient design with shorter phase change time in solidification procedure was related to circular finned tube. Numerically, the melting of RT82 by mixing various concentrations of Al₂O₃ in a cavity with one hot wall was reported by Arasu and Mujumdar [59]. Utilization of two forms of tree formed fins has been simulated by Sciacovelli et al. [60] for optimizing and reaching the maximum efficiency for LHTES system. As a result, there are various published scientific works expressing the importance of shape of fin in order to augment the performance of units. Numerically, the solidification procedure in a horizontal cylinder with PCM was studied by Ismail et al. [61] who found that the time of PCM solidification plummeted when the inlet fluid temperature decreased. To reduce cost of experimental procedure, various numerical approaches were suggested [62–79]. The charging treatment of PCM has been illustrated by Xiaohu et al. [80] who conducted the tests at 0°, 30°, 60° and 90° inclination. In comparison with the case at 90°, the melting duration decreased by 12.28% at 0°, 22.81% at 30° and 34.21% at 60°. The impact of inlet mass stream rate and water temperature on heat storage and thermal efficiency in a tube was investigated by Tao and He [81]. Based on their results, raising the HTF mass stream and temperature increases the rate of melting. Additionally, raising the number of tubes augments the efficiency of the heat exchanger.

In current modeling, charging of paraffin within a square enclosure was simulated. Spiral pipe was used in which hot fluid flows and converts the solid PCM to liquid. To augment PCM’s thermal conductivity within charging procedure, nanopowders have been dispersed. Nanoparticles were utilized in both hot water and paraffin. FVM was selected to simulate, and outputs were demonstrated in various stages.

2 Enclosure with spiral pipe

As depicted in Fig. 1, to charge the paraffin inside a square tank, a spiral pipe was employed. Water with impose of nanoparticles was considered as testing fluid inside the spiral pipe. The reason of selecting paraffin is its high capacity to store energy and to improve its thermal feature; CuO was added in it as utilized in Ref. [82]. To model this problem, we use the below equations:

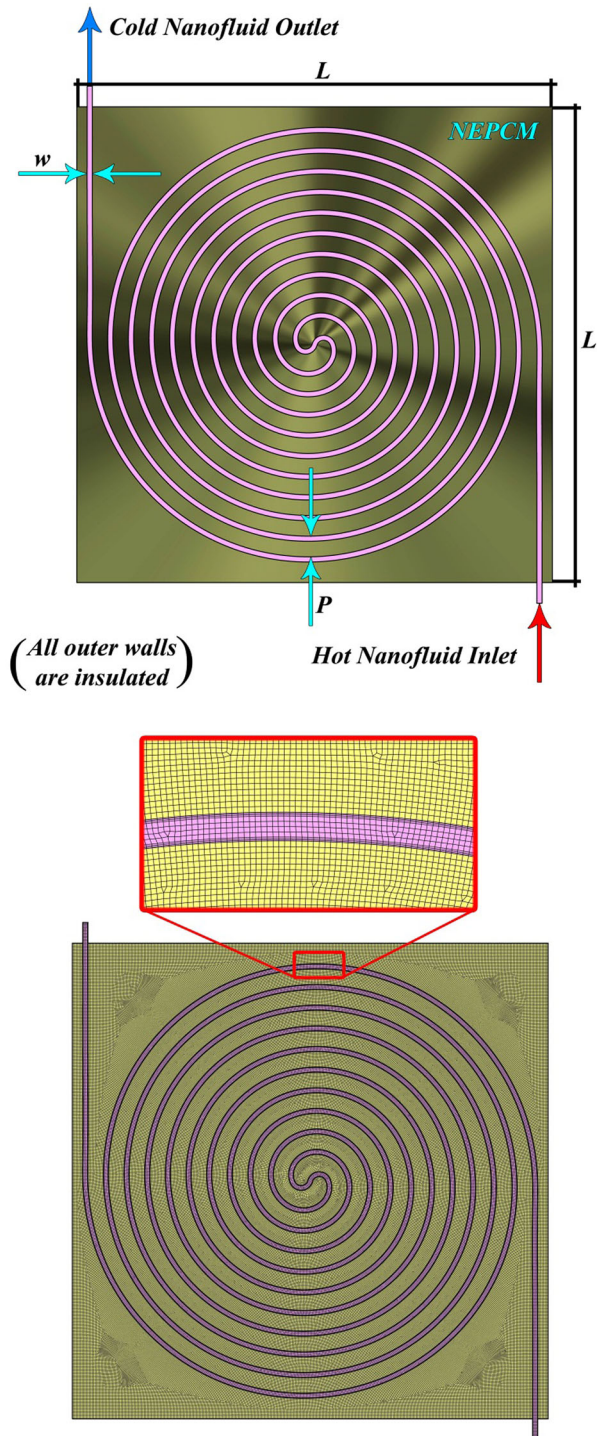
$$\nabla \cdot \vec{V} = 0 \tag{1}$$

$$\frac{\partial u}{\partial t} + \vec{V} \cdot \nabla u = \frac{1}{\rho_{nf}} (-\nabla P + \mu_{nf} \nabla^2 u) + C u \frac{(1 - \lambda)^2}{\lambda^3 + \varepsilon}, \quad C = 10^5, \quad \varepsilon = 10^{-3} \tag{2}$$

$$\frac{\partial v}{\partial t} + \vec{V} \cdot \nabla v = \frac{1}{\rho_{nf}} (-\nabla P + \mu_{nf} \nabla^2 v) + C v \frac{(1 - \lambda)^2}{\lambda^3 + \varepsilon} + g(T - T_{ref})(\rho\beta)_{nf} \tag{3}$$

$$\frac{\partial T}{\partial t} + \vec{V} \cdot \nabla T = -\frac{\partial(\rho L\lambda)_{nf}}{\partial t} + \frac{k_{nf}}{(\rho C_p)_{nf}} \nabla^2 T \tag{4}$$

Fig. 1 Spiral unit and mesh



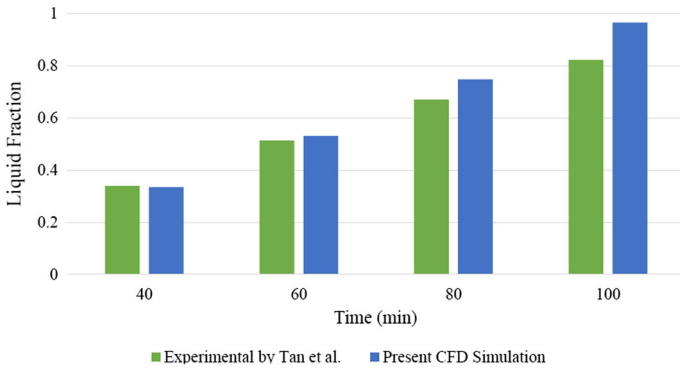


Fig. 2 Comparison of outputs with Ref. [28]

The last term of Eq. (3) appears with use of Boussinesq approximation. To include the impact of nanoparticles, homogeneous model was used as mentioned in [82] and also for hot fluid section, we utilized hybrid nanoparticles. For mixture of water with hybrid nanopowders, same formula of [83] was utilized.

The sensible and total enthalpies are:

$$h = h_{ref} + \int_{T_{ref}}^T (C_p)_{nf} dT \tag{5}$$

$$H_e = h + \lambda L \tag{6}$$

where h_{ref} is the enthalpy at $T_{ref} = 273$ K.

λ should be obtained from the below formula:

$$\lambda = \begin{cases} \frac{T_s - T}{T_s - T_i} & T_s < T < T_l \\ 0 & T < T_s \\ 1 & T < T_l \end{cases} \tag{7}$$

Mesh sample is shown in Fig. 1 and to obtain better convergence, structure grid was utilized. Enthalpy–porosity method which is defined in ANSYS FLUENT was employed in this article [82]. For pressure correction, we utilized PRESTO algorithm.

3 Results and discussion

In current article, to improve the melting inside a tank, a spiral pipe was added in which hot fluid flows and helps with melting process. FVM was applied to simulate this process, and verification in view of values of liquid fraction is demonstrated in Fig. 2. As depicted, nice agreement with Ref. [84] was obtained and it proves the accuracy of current code. Distributions of temperature for various parts are depicted in Fig. 3 when $Re = 500$. Fluid inside the spiral pipe becomes colder and makes the solid paraffin to melt. As time progress, the liquid parts appear, and in this zone, the buoyancy force helps to faster melting. So, outlet temperature of fluid reduces when exiting the spiral. It is obvious that NEPCM domain has lower temperature in comparison with fluid inside the spiral. Temperature of nanofluid augments till time progresses to $t = 10$ min. Also, T_{NEPCM} zone reaches to constant value after melting becomes completed.

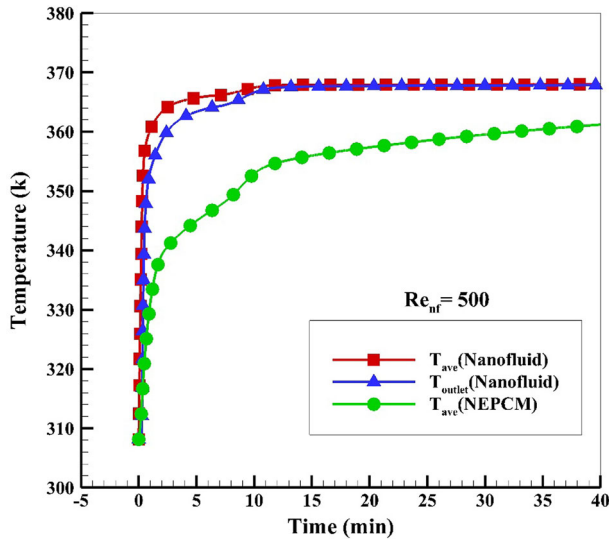


Fig. 3 Temperature distribution history in various parts

This type of system is very common in industry due to its easier cleaning of HTF pipes. Nanopowders were dispersed to augment thermal behavior (not only in fluid flows in pipe but also in PCM). Figures 4, 5 and 6 illustrate the velocity, $S_{gen,f}$ and $S_{gen,th}$ contours when $Re = 500$. In addition, we increased the Re to 1000 and extracted the contours as depicted in Figs. 7, 8 and 9. The main goal of designers is reaching to lowest irreversibility, and by finding these regions with greater entropy during process, they can remove that fault. Buoyancy force acts in this process and affects the speed of melting. In initial time, the hot nanomaterial in pipe creates the great flux and affects the boundaries, and after about 5 min, the heat flux reaches to its highest values and then reduces and finally reaches to constant value. Due to jump in velocity gradient in initial time ($t < 5\text{min}$), $S_{gen,f}$ increases suddenly and then decreases. As time progresses, eddies generate near the outer side of spiral which provide greater temperature gradient and lower $S_{gen,th}$. Augmenting inlet velocity makes heat flux to decrease which creates stronger temperature gradient, and more thermal irreversibility appears in contours. Increasing pumping power has no sensible effect in greater time, while it has supportive effect in middle time of process. Velocity and $S_{gen,f}$ have direct relation in view of regions with greater values because the main term of frictional irreversibility is velocity gradient. As depicted in contours of $t = 5\text{min}$, the uniform distribution of $S_{gen,th}$ exists in this time. Melting starts from inner spiral, and the outer side was the last regions which convert from solid to liquid. The zone near the below wall takes more time to melt because in this region, free convection is poor.

4 Conclusion

Spiral heat exchanger is employed inside a tank to accelerate melting process. To rise the thermal behavior of PCM and H_2O , nanopowders are dispersed in both of them. The focus of this research is irreversibility of NEPCM during charging. Results indicate that heat flux which affects the NEPCM has sudden increment at initial time, but it reduces with progress of time.

Fig. 4 Contours of velocity, $S_{gen,f}$ and $S_{gen,th}$ when $Re = 500, t = 5 \text{ min}$

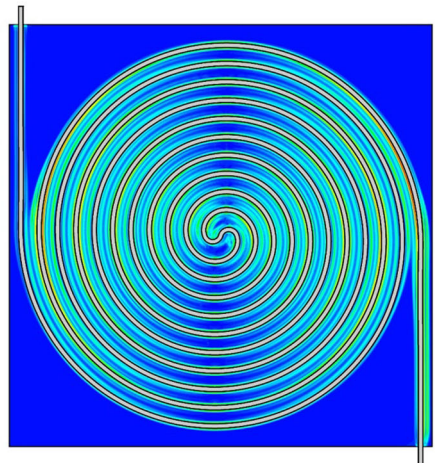
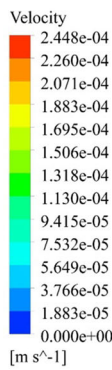
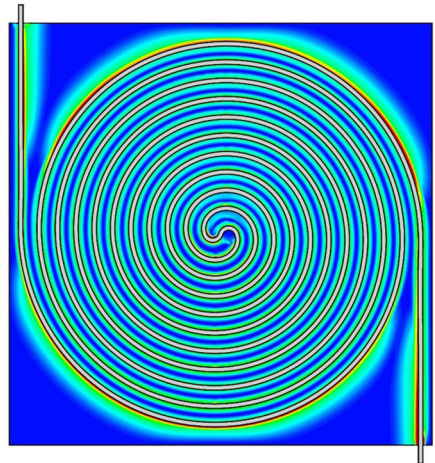
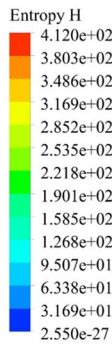
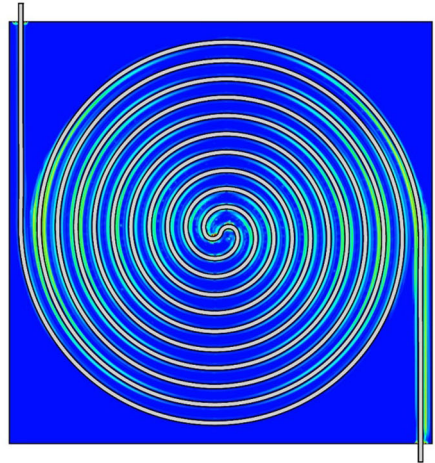
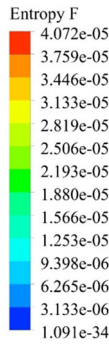


Fig. 5 Contours of velocity, $S_{gen,f}$ and $S_{gen,th}$ when $Re = 500, t = 20 \text{ min}$

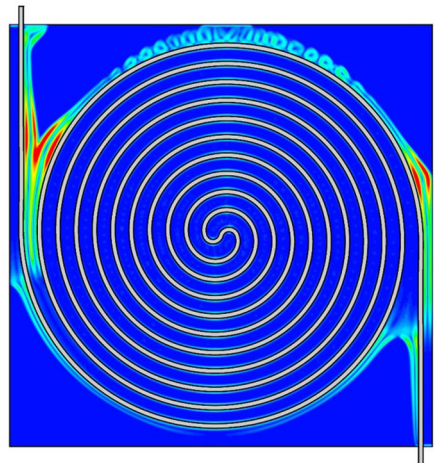
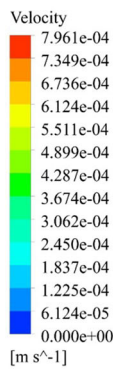
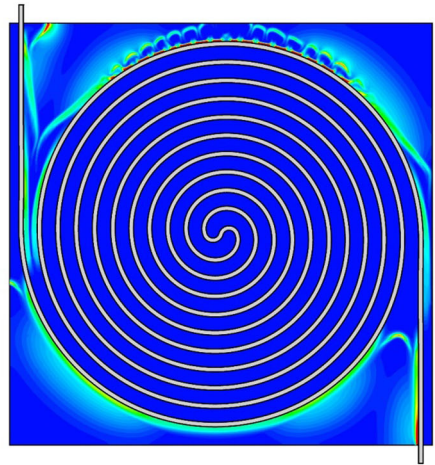
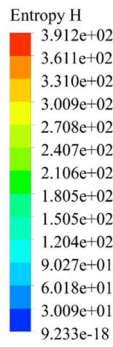
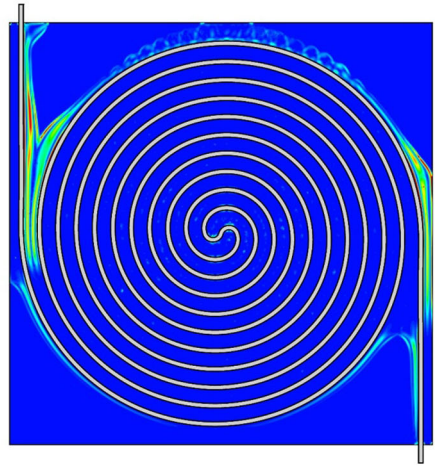
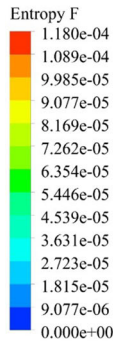


Fig. 6 Contours of velocity, $S_{gen,f}$ and $S_{gen,th}$ when $Re = 500, t = 80 \text{ min}$

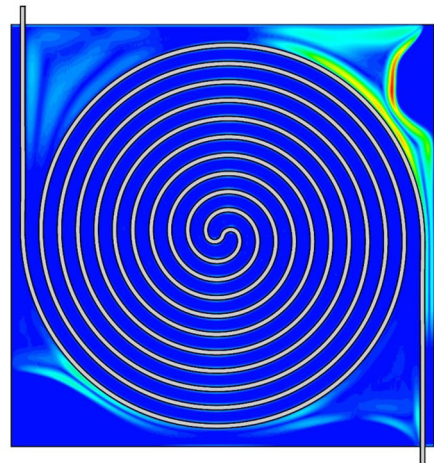
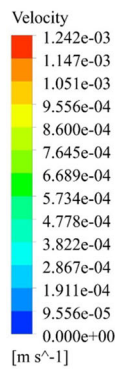
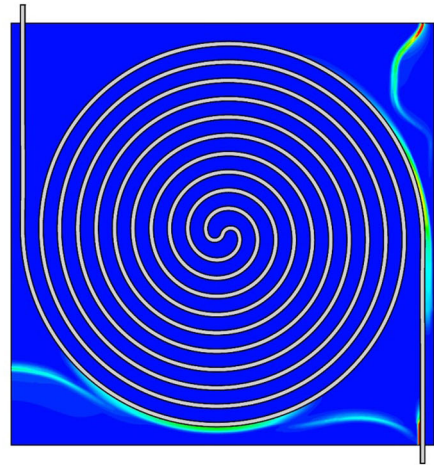
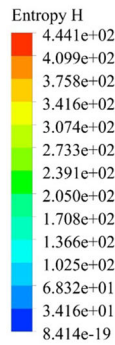
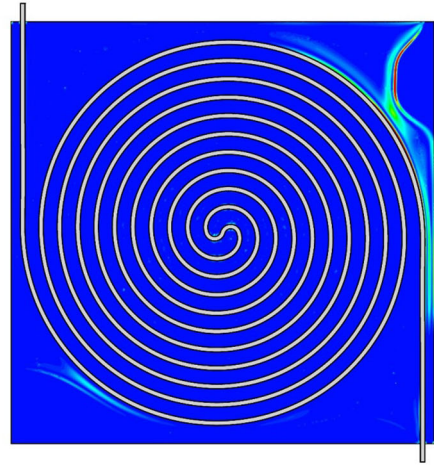
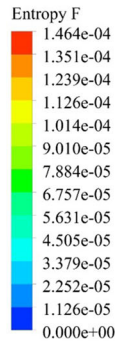


Fig. 7 Contours of velocity, $S_{gen,f}$ and $S_{gen,th}$ when $Re = 1000, t = 5 \text{ min}$

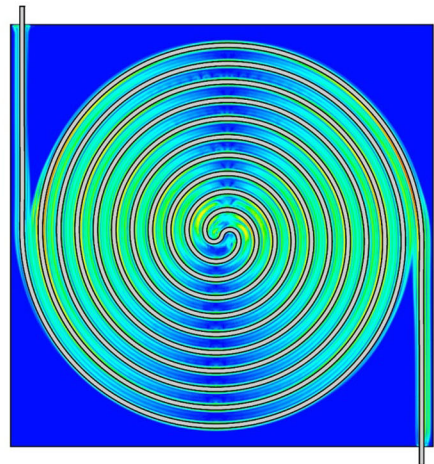
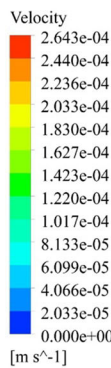
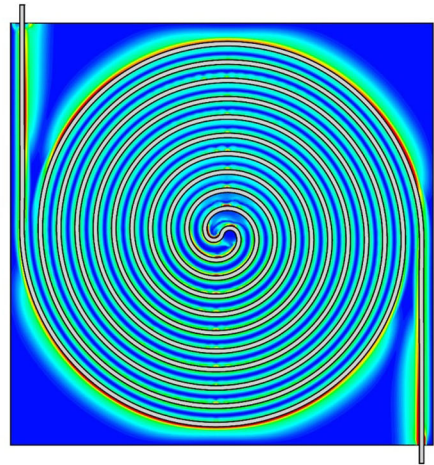
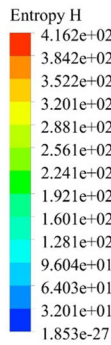
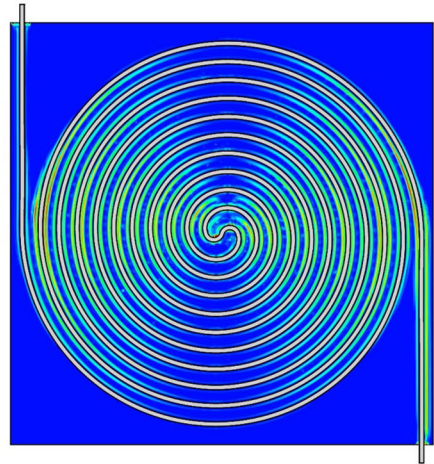
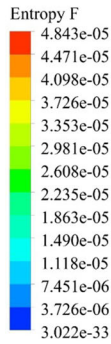


Fig. 8 Contours of velocity, $S_{gen,f}$ and $S_{gen,th}$ when $Re = 1000, t = 20 \text{ min}$

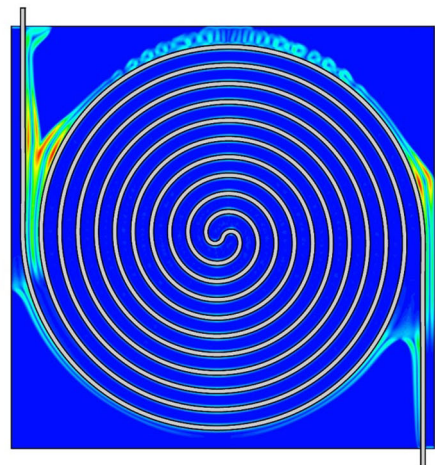
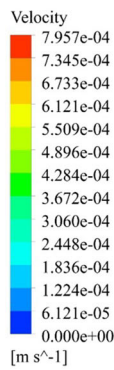
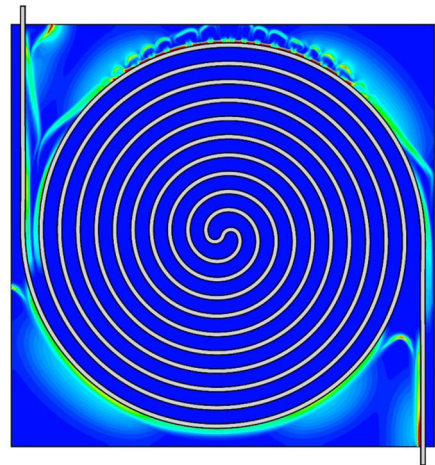
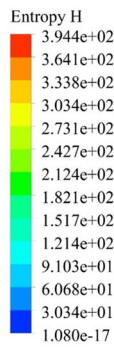
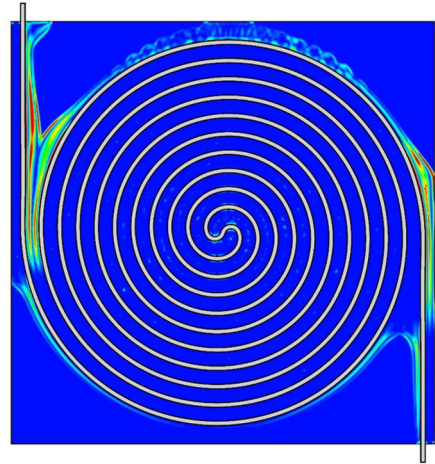
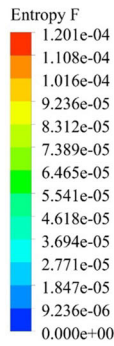
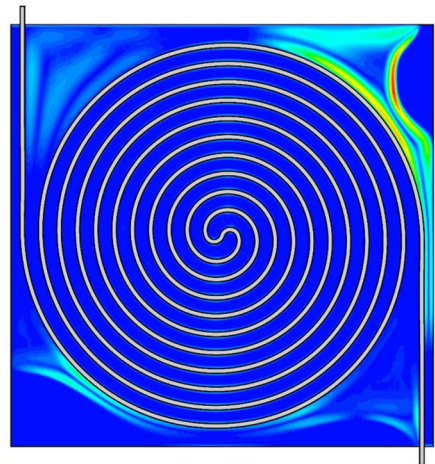
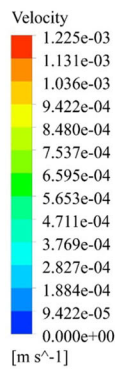
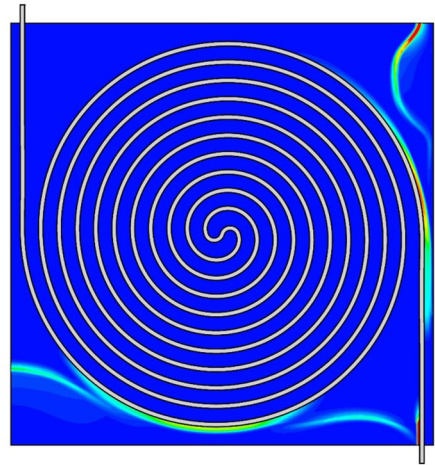
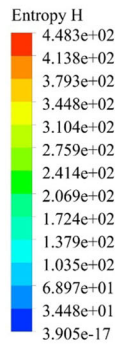
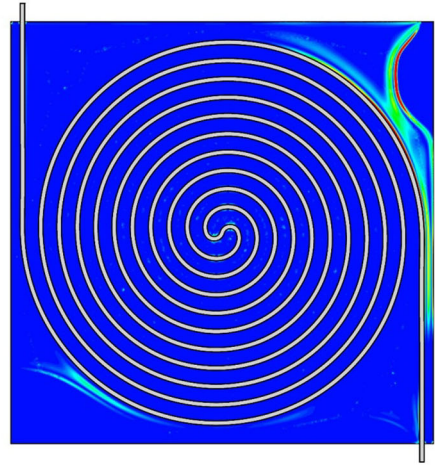
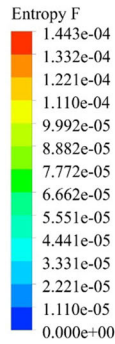


Fig. 9 Contours of velocity, $S_{gen,f}$ and $S_{gen,th}$ when $Re = 1000$, $t = 80$ min



Thermal irreversibility reduces during charging which attributes to increasing temperature of NEPCM.

Acknowledgements The authors extend their appreciation to the Deanship of Scientific Research at King Khalid University for funding this article through Research Groups Program under Grant Number (R.G. P2./66/40).

References

1. M. Sheikholeslami, A. Ghasemi, Solidification heat transfer of nanofluid in existence of thermal radiation by means of FEM. *Int. J. Heat Mass Transf.* **123**, 418–431 (2018)
2. M. Sheikholeslami, Numerical simulation for solidification in a LHTESS by means of nano-enhanced PCM. *J. Taiwan Inst. Chem. Eng.* **86**, 25–41 (2018)
3. M. Sheikholeslami, R. Haq, A. Shafee, Z. Li, Y.G. Elaraki, I. Tlili, Heat transfer simulation of heat storage unit with nanoparticles and fins through a heat exchanger. *Int. J. Heat Mass Transf.* **135**, 470–478 (2019)
4. M. Sheikholeslami, R. Haq, A. Shafee, Z. Li, Heat transfer behavior of nanoparticle enhanced PCM solidification through an enclosure with V shaped fins. *Int. J. Heat Mass Transf.* **130**, 1322–1342 (2019)
5. M. Sheikholeslami, M.K. Sadoughi, Simulation of CuO- water nanofluid heat transfer enhancement in presence of melting surface. *Int. J. Heat Mass Transf.* **116**, 909–919 (2018)
6. S.A. Farshad, M. Sheikholeslami, Turbulent nanofluid flow through a solar collector influenced by multi-channel twisted tape considering entropy generation. *Eur. Phys. J. Plus* **134**, 149 (2019). <https://doi.org/10.1140/epjp/i2019-12606-2>
7. Z. Li, M. Sheikholeslami, A.S. Mittal, A. Shafee, R. Haq, Nanofluid heat transfer in a porous duct in existence of Lorentz forces using Lattice Boltzmann method. *Eur. Phys. J. Plus* **134**, 30 (2019). <https://doi.org/10.1140/epjp/i2019-12406-8>
8. L. Yang, M. Mao, J.N. Huang, W. Ji, Enhancing the thermal conductivity of SAE 50 engine oil by adding zinc oxide nano-powder: an experimental study. *Powder Technol.* **356**, 335–341 (2019)
9. M. Sheikholeslami, Numerical approach for MHD Al₂O₃-water nanofluid transportation inside a permeable medium using innovative computer method. *Comput. Methods Appl. Mech. Eng.* **344**, 306–318 (2019)
10. M. Sheikholeslami, B. Rezaeianjouybari, M. Darzi, A. Shafee, Z. Li, T.K. Nguyen, Application of nano-refrigerant for boiling heat transfer enhancement employing an experimental study. *Int. J. Heat Mass Transf.* **141**, 974–980 (2019)
11. N.A. Sheikh, F. Ali, M. Saqib, I. Khan, S.A.A. Jan, *Eur. Phys. J. Plus* **132**, 54 (2017)
12. M. Sheikholeslami, Application of Darcy law for nanofluid flow in a porous cavity under the impact of Lorentz forces. *J. Mol. Liq.* **266**, 495–503 (2018)
13. F. Mabood, S. Shateyi, A. Khan, *Eur. Phys. J. Plus* **130**, 188 (2015)
14. B. Rezaeianjouybari, M. Sheikholeslami, A. Shafee, H. Babazadeh, A novel Bayesian optimization for flow condensation enhancement using nanorefrigerant: a combined analytical and experimental study. *Chem. Eng. Sci.* **215**, 115465 (2020)
15. M. Sheikholeslami, New computational approach for exergy and entropy analysis of nanofluid under the impact of Lorentz force through a porous media. *Comput. Methods Appl. Mech. Eng.* **344**, 319–333 (2019)
16. M. Sheikholeslami, H.B. Rokni, Magnetic nanofluid natural convection in the presence of thermal radiation considering variable viscosity. *Eur. Phys. J. Plus* **132**, 238 (2017). <https://doi.org/10.1140/epjp/i2017-11498-4>
17. M. Sheikholeslami, M.M. Bhatti, Active method for nanofluid heat transfer enhancement by means of EHD. *Int. J. Heat Mass Transf.* **109**, 115–122 (2017)
18. M. Sheikholeslami, M.A. Sheremet, A. Shafee, I. Tlili, Simulation of nanoliquid thermogravitational convection within a porous chamber imposing magnetic and radiation impacts. *Phys. A Stat. Mech. Appl.* (2020). <https://doi.org/10.1016/j.physa.2019.124058>
19. M. Sheikholeslami, R. Ellahi, Three dimensional mesoscopic simulation of magnetic field effect on natural convection of nanofluid. *Int. J. Heat Mass Transf.* **89**, 799–808 (2015)
20. M. Sheikholeslami, H.B. Rokni, Melting heat transfer influence on nanofluid flow inside a cavity in existence of magnetic field. *Int. J. Heat Mass Transf.* **114**, 517–526 (2017)
21. M. Sheikholeslami, Finite element method for PCM solidification in existence of CuO nanoparticles. *J. Mol. Liq.* **265**, 347–355 (2018)

22. M. Sheikholeslami, Solidification of NEPCM under the effect of magnetic field in a porous thermal energy storage enclosure using CuO nanoparticles. *J. Mol. Liq.* **263**, 303–315 (2018)
23. M. Sheikholeslami, Z. Li, A. Shafee, Lorentz forces effect on NEPCM heat transfer during solidification in a porous energy storage system. *Int. J. Heat Mass Transf.* **127**, 665–674 (2018)
24. M. Sheikholeslami, A. Ghasemi, Z. Li, A. Shafee, S. Saleem, Influence of CuO nanoparticles on heat transfer behavior of PCM in solidification process considering radiative source term. *Int. J. Heat Mass Transf.* **126**, 1252–1264 (2018)
25. M. Sheikholeslami, Numerical modeling of nano enhanced PCM solidification in an enclosure with metallic fin. *J. Mol. Liq.* **259**, 424–438 (2018)
26. Z. Li, M. Sheikholeslami, Z. Shah, A. Shafee, A.-R. Al-Qawasm, I. Tlili, Transient process in a finned triplex tube during phase changing of aluminum oxide enhanced PCM. *Eur. Phys. J. Plus* **134**, 173 (2019). <https://doi.org/10.1140/epjp/i2019-12627-9>
27. M. Sheikholeslami, O. Mahian, Enhancement of PCM solidification using inorganic nanoparticles and an external magnetic field with application in energy storage systems. *J. Clean. Prod.* **215**, 963–977 (2019)
28. F. Agyenim, P. Eames, M. Smyth, Heat transfer enhancement in medium temperature thermal energy storage system using a multitube heat transfer array. *Renew. Energy* **35**(1), 198–207 (2010)
29. M. Sheikholeslami, Influence of magnetic field on nanofluid free convection in an open porous cavity by means of Lattice Boltzmann Method. *J. Mol. Liq.* **234**, 364–374 (2017)
30. Y. Qin, H. He, A new simplified method for measuring the albedo of limited extent targets. *Sol. Energy* **157**(Supplement C), 1047–1055 (2017)
31. M. Sheikholeslami, Influence of magnetic field on $\text{Al}_2\text{O}_3\text{-H}_2\text{O}$ nanofluid forced convection heat transfer in a porous lid driven cavity with hot sphere obstacle by means of LBM. *J. Mol. Liq.* **263**, 472–488 (2018)
32. L. Yang, J. Xu, K. Du, X. Zhang, Recent developments on viscosity and thermal conductivity of nanofluids. *Powder Technol.* **317**, 348–369 (2017)
33. M. Sheikholeslami, S.A. Shehzad, Simulation of water based nanofluid convective flow inside a porous enclosure via non-equilibrium model. *Int. J. Heat Mass Transf.* **120**, 1200–1212 (2018)
34. M. Sheikholeslami, M. Seyednezhad, Simulation of nanofluid flow and natural convection in a porous media under the influence of electric field using CVFEM. *Int. J. Heat Mass Transf.* **120**, 772–781 (2018)
35. Y. Qin, Y. He, B. Wu, S. Ma, X. Zhang, Regulating top albedo and bottom emissivity of concrete roof tiles for reducing building heat gains. *Energy Build.* **156**(Supplement C), 218–224 (2017)
36. M. Sheikholeslami, Magnetic field influence on $\text{CuO-H}_2\text{O}$ nanofluid convective flow in a permeable cavity considering various shapes for nanoparticles. *Int. J. Hydrogen Energy* **42**, 19611–19621 (2017)
37. M. Sheikholeslami, S.A. Shehzad, CVFEM simulation for nanofluid migration in a porous medium using Darcy model. *Int. J. Heat Mass Transf.* **122**, 1264–1271 (2018)
38. M. Sheikholeslami, M. Darzi, M.K. Sadoughi, Heat transfer improvement and pressure drop during condensation of refrigerant-based Nanofluid. *Exp. Proced. Int. J. Heat Mass Transf.* **122**, 643–650 (2018)
39. Y. Qin, Pavement surface maximum temperature increases linearly with solar absorption and reciprocal thermal inertial. *Int. J. Heat Mass Transf.* **97**, 391–399 (2016)
40. M. Sheikholeslami, Numerical investigation of nanofluid free convection under the influence of electric field in a porous enclosure. *J. Mol. Liq.* **249**, 1212–1221 (2018)
41. M. Sheikholeslami, CuO-water nanofluid flow due to magnetic field inside a porous media considering Brownian motion. *J. Mol. Liq.* **249**, 921–929 (2018)
42. M. Sheikholeslami, Numerical investigation for $\text{CuO-H}_2\text{O}$ nanofluid flow in a porous channel with magnetic field using mesoscopic method. *J. Mol. Liq.* **249**, 739–746 (2018)
43. Y. Qin, J. Liang, K. Tan, F. Li, A side by side comparison of the cooling effect of building blocks with retro-reflective and diffuse-reflective walls. *Sol. Energy* **133**, 172–179 (2016)
44. M. Sheikholeslami, S.A. Shehzad, Numerical analysis of $\text{Fe}_3\text{O}_4\text{-H}_2\text{O}$ nanofluid flow in permeable media under the effect of external magnetic source. *Int. J. Heat Mass Transf.* **118**, 182–192 (2018)
45. M. Sheikholeslami, H.B. Rokni, Numerical simulation for impact of Coulomb force on nanofluid heat transfer in a porous enclosure in presence of thermal radiation. *Int. J. Heat Mass Transf.* **118**, 823–831 (2018)
46. Y. Qin, J. Liang, H. Yang, Z. Deng, Gas permeability of pervious concrete and its implications on the application of pervious pavements. *Measurement* **78**, 104–110 (2016)
47. M. Sheikholeslami, S.A. Shehzad, CVFEM for influence of external magnetic source on $\text{Fe}_3\text{O}_4\text{-H}_2\text{O}$ nanofluid behavior in a permeable cavity considering shape effect. *Int. J. Heat Mass Transf.* **115**, 180–191 (2017)
48. M. Sheikholeslami, M. Seyednezhad, Nanofluid heat transfer in a permeable enclosure in presence of variable magnetic field by means of CVFEM. *Int. J. Heat Mass Transf.* **114**, 1169–1180 (2017)
49. Y. Qin, J.E. Hiller, Understanding pavement-surface energy balance and its implications on cool pavement development. *Energy Build.* **85**, 389–399 (2014)

50. M. Sheikholeslami, M. Sadoughi, Mesoscopic method for MHD nanofluid flow inside a porous cavity considering various shapes of nanoparticles. *Int. J. Heat Mass Transf.* **113**, 106–114 (2017)
51. M. Sheikholeslami, M.M. Bhatti, Forced convection of nanofluid in presence of constant magnetic field considering shape effects of nanoparticles. *Int. J. Heat Mass Transf.* **111**, 1039–1049 (2017)
52. Y. Qin, M. Zhang, G. Mei, A new simplified method for measuring the permeability characteristics of highly porous media. *J. Hydrol.* **562**, 725–732 (2018)
53. M. Sheikholeslami, S.A. Shehzad, Thermal radiation of ferrofluid in existence of Lorentz forces considering variable viscosity. *Int. J. Heat Mass Transf.* **109**, 82–92 (2017)
54. M. Sheikholeslami, H.B. Rokni, Nanofluid two phase model analysis in existence of induced magnetic field. *Int. J. Heat Mass Transf.* **107**, 288–299 (2017)
55. Y. Qin, Urban canyon albedo and its implication on the use of reflective cool pavements. *Energy Build.* **96**, 86–94 (2015)
56. M. Sheikholeslami, S.A. Farshad, A. Shafee, I. Tlili, Modeling of solar system with helical swirl flow device considering nanofluid turbulent forced convection. *Phys. A Stat. Mech. Appl.* (2020). <https://doi.org/10.1016/j.physa.2019.123952>
57. M. Sheikholeslami, A. Nematpour Keshteli, H. Babazadeh, Nanoparticles favorable effects on performance of thermal storage units. *J. Mol. Liq.* **300**, 112329 (2020)
58. N.H.S. Tay, F. Bruno, M. Belusko, Comparison of pinned and finned tubes in a phase change thermal energy storage system using CFD. *Appl. Energy* **104**, 86–79 (2013)
59. A.V. Arasu, A.S. Mujumdar, Numerical study on melting of paraffin wax with Al_2O_3 in a square enclosure. *Int. Commun. Heat Mass Transf.* **39**, 8–16 (2012)
60. A. Sciacovelli, F. Gagliardi, V. Verda, Maximization of performance of a PCM latent heat storage system with innovative fins. *Appl. Energy* **137**, 715–707 (2015)
61. K.A.R. Ismail, F.A.M. Lino, R.C.R. da Silva, A.B. de Jesus, L.C. Paixao, Experimentally validated two dimensional numerical model for the solidification of PCM along a horizontal long tube. *Int. J. Therm. Sci.* **75**, 184–193 (2014)
62. Y. Qin, H. He, X. Ou, T. Bao, Experimental study on darkening water-rich mud tailings for accelerating desiccation. *J. Clean. Prod.* (2019). <https://doi.org/10.1016/j.jclepro.2019.118235>
63. M. Sheikholeslami, H.B. Rokni, Simulation of nanofluid heat transfer in presence of magnetic field: a review. *Int. J. Heat Mass Transf.* **115**, 1203–1233 (2017)
64. Y. Qin, J.E. Hiller, D. Meng, Linearity between pavement thermophysical properties and surface temperatures. *J. Mater. Civ. Eng.* (2019). [https://doi.org/10.1061/\(ASCE\)MT.1943-5533.0002890](https://doi.org/10.1061/(ASCE)MT.1943-5533.0002890)
65. M. Sheikholeslami, H.B. Rokni, Magnetic nanofluid flow and convective heat transfer in a porous cavity considering Brownian motion effects. *Phys. Fluids* (2018). <https://doi.org/10.1063/1.5012517>
66. Y. Qin, J. Luo, Z. Chen, G. Mei, L.-E. Yan, Measuring the albedo of limited-extent targets without the aid of known-albedo masks. *Sol. Energy* **171**, 971–976 (2018)
67. L. Yang, K. Du, A comprehensive review on the natural, forced and mixed convection of non-Newtonian fluids (nanofluids) inside different cavities. *J. Thermal Anal. Calorim.* 2019, In press. <https://doi.org/10.1007/s10973-019-08987-y>
68. M. Sheikholeslami, M. Jafaryar, A. Shafee, Z. Li, R. Haq, Heat transfer of nanoparticles employing innovative turbulator considering entropy generation. *Int. J. Heat Mass Transf.* **136**, 1233–1240 (2019)
69. M. Sheikholeslami, M. Jafaryar, M. Hedayat, A. Shafee, Z. Li, T.K. Nguyen, M. Bakouri, Heat transfer and turbulent simulation of nanomaterial due to compound turbulator including irreversibility analysis. *Int. J. Heat Mass Transf.* **137**, 1290–1300 (2019)
70. Y. Qin, A review on the development of cool pavements to mitigate urban heat island effect. *Renew. Sustain. Energy Rev.* **52**, 445–459 (2015)
71. Y. Qin, Y. He, J.E. Hiller, G. Mei, A new water-retaining paver block for reducing runoff and cooling pavement. *J. Clean. Prod.* **199**, 948–956 (2018)
72. M. Sheikholeslami, M. Jafaryar, Z. Li, Nanofluid turbulent convective flow in a circular duct with helical turbulators considering CuO nanoparticles. *Int. J. Heat Mass Transf.* **124**, 980–989 (2018)
73. M. Sheikholeslami, S.A. Shehzad, Z. Li, Water based nanofluid free convection heat transfer in a three dimensional porous cavity with hot sphere obstacle in existence of Lorenz forces. *Int. J. Heat Mass Transf.* **125**, 375–386 (2018)
74. M. Sheikholeslami, M. Darzi, Z. Li, Experimental investigation for entropy generation and exergy loss of nano-refrigerant condensation process. *Int. J. Heat Mass Transf.* **125**, 1087–1095 (2018)
75. Y. Qin, Y. Zhao, X. Chen, L. Wang, F. Li, T. Bao, Moist curing increases the solar reflectance of concrete. *Constr. Build. Mater.* **215**, 114–118 (2019)
76. M. Sheikholeslami, S.A. Shehzad, Z. Li, A. Shafee, Numerical modeling for alumina nanofluid magneto-hydrodynamic convective heat transfer in a permeable medium using Darcy law. *Int. J. Heat Mass Transf.* **127**, 614–622 (2018)

77. M. Sheikholeslami, M. Jafaryar, S. Saleem, Z. Li, A. Shafee, Y. Jiang, Nanofluid heat transfer augmentation and exergy loss inside a pipe equipped with innovative turbulators. *Int. J. Heat Mass Transf.* **126**, 156–163 (2018)
78. Y. Qin, M. Zhang, J.E. Hiller, Theoretical and experimental studies on the daily accumulative heat gain from cool roofs. *Energy* **129**, 138–147 (2017)
79. M. Sheikholeslami, Lattice Boltzmann Method simulation of MHD non-Darcy nanofluid free convection. *Phys. B* **516**, 55–71 (2017)
80. Y. Xiaohu, G. Zengxu, L. Yanhua, J. Liwen, H. Ya-Ling, Effect of inclination on the thermal response of composite phase change materials for thermal energy storage. *Appl. Energy* **238**, 33–22 (2019)
81. Y. Tao, Y. He, Numerical study on thermal energy storage performance of phase change material under non-steady-state inlet boundary. *Appl. Energy* **88**(11), 4172–4179 (2011)
82. X. Ma, M. Sheikholeslami, M. Jafaryar, A. Shafee, T. Nguyen-Thoi, Z. Li, Solidification inside a clean energy storage unit utilizing phase change material with copper oxide nanoparticles. *J. Clean. Prod.* **245**, 118888 (2020). <https://doi.org/10.1016/j.jclepro.2019.118888>
83. M. Sheikholeslami, S.A.M. Mehryan, A. Shafee, M.A. Sheremet, Variable magnetic forces impact on magnetizable hybrid nanofluid heat transfer through a circular cavity. *J. Mol. Liq.* **277**, 388–396 (2019)
84. F.L. Tan, S.F. Hosseinizadeh, J.M. Khodadadi, L. Fan, *Int. J. Heat Mass Transf.* **52**, 3464–3472 (2009)